Journal Pre-proofs

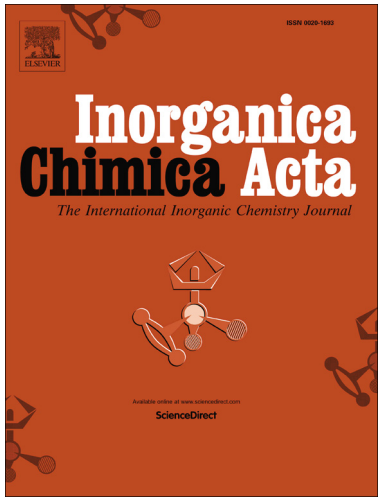

Research paper

Di-μ-oxidovanadium(V) di-nuclear complexes: Synthesis, X-ray, DFT modeling, Hirshfeld surface analysis and Antioxidant activity

Ali Hasnaoui, Ismail Hdoufane, Abderrahim Alahyane, Abdallah Nayad, Driss Cherqaoui, Mustapha Ait Ali, Larbi El Firdoussi

PII: S0020-1693(19)30860-6
DOI: https://doi.org/10.1016/j.ica.2019.119276
Reference: ICA 119276

To appear in: *Inorganica Chimica Acta*

Received Date: 5 July 2019
Revised Date: 8 November 2019
Accepted Date: 10 November 2019

Please cite this article as: A. Hasnaoui, I. Hdoufane, A. Alahyane, A. Nayad, D. Cherqaoui, M. Ait Ali, L. El Firdoussi, Di-μ-oxidovanadium(V) di-nuclear complexes: Synthesis, X-ray, DFT modeling, Hirshfeld surface analysis and Antioxidant activity, *Inorganica Chimica Acta* (2019), doi: https://doi.org/10.1016/j.ica.2019.119276

Di-μ-oxidovanadium(V) di-nuclear complexes: Synthesis, X-ray, DFT modeling, Hirshfeld surface analysis and Antioxidant activity

Ali Hasnaoui [1], Ismail Hdoufane [2], Abderrahim Alahyane [3], Abdallah Nayad [1], Driss Cherqaoui [2], Mustapha Ait Ali [1] and Larbi El Firdoussi [1*]

[1] Equipe de Chimie de Coordination et de Catalyse, Département de Chimie, Université Cadi Ayyad, Faculté des Sciences Semlalia, BP 2390, Marrakech, Morocco ;
[2] Laboratory of Molecular Chemistry, Department of Chemistry, Faculty of Sciences Semlalia, Cadi Ayyad University of Marrakech, BP 2390, Morocco;
[3] Food Sciences Laboratory, Department of Biology, Faculty of Sciences-Semlalia, Cadi Ayyad University of Marrakech, P.O. Box 2390, Morocco.

ABSTRACT

In this work, two di-μ-oxidovanadium(V) complexes, $[(L_1H)VO(\mu\text{-}O)]_2$ (**C1**) and $[(L_2H)VO(\mu\text{-}O)]_2$ (**C2**), with tridentate Schiff base ligands, [N-(2-hydroxyethylamino)ethyl]-5-methoxysalicylaldimine (L_1H) and 2-[(2-(2-Hydroxyethylamino) ethylimino)methyl] phenol (L_2H), respectively, were prepared and characterized by various spectroscopic techniques. The X-ray diffraction of **C1** showed six-coordinate vanadium in a distorted octahedral geometry with the imine, phenolate and amine donors of the ligand and two oxo-group bonds. Density functional theory (DFT) was carried out using B3LYP level with the 6-31G basis set in order to predict the molecular structure of **C1**, delineate its vibrational wavenumbers and define the theoretical NMR shifts, which were performed with the GIAO approach. Thereafter, Hirshfeld surface (HS) and 2D fingerprint analysis were used to investigate the intermolecular contacts in the **C1** complex. The DPPH free radical scavenging assay was used to evaluate the antioxidant activity of both **C1** and **C2** complexes.

Keywords: Vanadium complexes; X-ray diffraction; DFT; Hirshfeld analysis; Antioxidant activity.

* Corresponding author: Prof. Larbi El Firdoussi (elfirdoussi@uca.ac.ma)

1. Introduction

Schiff bases constitute an important class of versatile ligands that can bind to metal ions forming metal complexes [1]. Their corresponding complexes have gained significant interest among scientists due to the existing range of applications, especially in the field of electrochemistry and catalysis [2–5]. Furthermore, they exhibit biological proprieties, such as antibacterial [6,7], anticancer [8,9], antifungal [10] and antioxidant activities [11,12].

The coordination chemistry of oxovanadium (IV), oxovanadium (V), and dioxovanadium (V) have attracted much attention and has been extensively studied due to its biological and therapeutic applications [13,14]. These elements are involved in a variety of biochemical processes including insulin-mimetic drugs [15,16], nitrogen fixation [17], anti-parasitic agents [18], haloperoxidation [19], and enzyme inhibition [15]. Numerous oxo and dioxovanadium complexes with Schiff base ligands are described in the literature [20], and their catalytic activity in oxidation has been investigated [21,22]. Also, many di-μ-oxidovanadium (V) compounds in a dimer symmetry with a methoxy or oxido group bridge were reported with NNO , NNS, and NOO donor ligands along with their biological and catalytic activities [23–32].

Quantum chemical calculations are known to be powerful approaches for the prediction of molecular structures and electronic properties [33]. They are widely used in the calculation of various spectroscopic characteristics such as vibrations, absorption, Raman and NMR spectra. They are also used in the understanding of reactions and the underlying kinetic profile and chemical mechanisms for organic and inorganic compounds [34] [35]. Several Vanadium complexes bearing Schiff bases were computed using the density functional theory DFT approach [36].

In the current work, we aim to extend our previous researches on Schiff base metal complexes [37] and to contribute to the discovery of effective and potent products with strong chemical and biological profile. To this end, a new di-oxovanadium (**C1**) in complex with [N-(2-hydroxyethylamino)ethyl]-5-methoxysalicylaldimine (L_1H) and an already described complex (**C2**) [38] were synthesized via one pot reaction. The structures of **C1** and **C2** were studied with the DFT method using the B3LYP/6-31G basis set. In addition, their intermolecular interactions were visualized and quantified using Hirshfeld Surface analysis and two-dimensional fingerprint plots. Thereafter, the antioxidant activity of **C1** and **C2** was tested using a DPPH free radical scavenging assay and compared with BHT and Quercetin (commercially available antioxidant products).

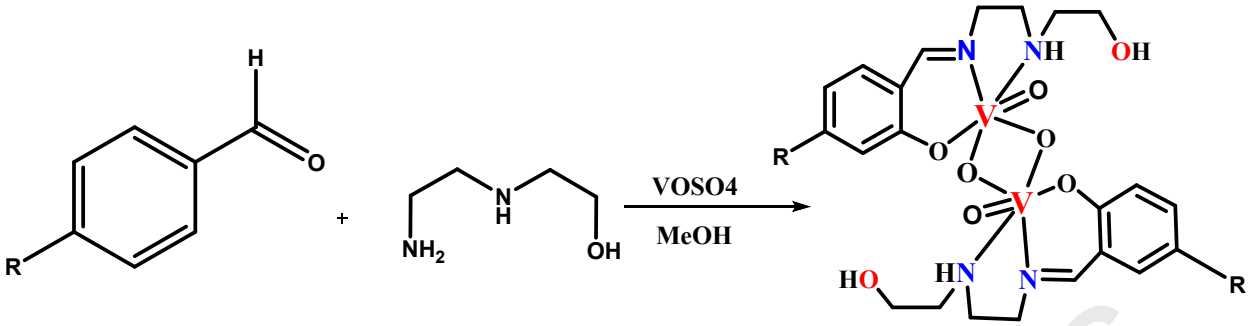

C1: R= OCH_3
C2: R= H

Scheme 1. Schematic synthesis of **C1** and **C2** complexes.

2. Experimental

2.1. Material and methods

$VOSO_4$, methanol, 2-((2-aminoethyl)amino)ethanol, 4-methoxysalicylaldehyde, DPPH, BHT, and Quercetin were purchased from Sigma Aldrich. NMR studies were recorded in DMSO-d_6 using a Bruker Avance 300 spectrometer. Chemical shifts are given in ppm relative to external TMS and coupling constants (*J*) are provided in Hz. FT-IR analysis was performed in KBr on a VERTEX 70.

2.2. Synthesis of oxovanadium complexes

For the complex **C1**, a mixture of 3-methoxysalicylaldehyde (100 mg, 0.66 mmol) and 2-((2-aminoethyl)amino)ethanol (68 mg, 0.66 mmol) in 15 mL of methanol was stirred at 70 °C during 15 min. Then, a solution of (106 mg, 0.66 mmol) $VOSO_4$ in methanol (5mL) was added dropwise to the mixture. After five hours of stirring, a yellow precipitate was obtained. The solid was filtered and washed with methanol. Recrystallization in CH_3OH/H_2O (8/2, v:v) afforded the **C1** product in 58% yield (0.23 g, 0.37 mmol). The same procedure was adopted to synthesize the **C2** complex in the presence of salicylic aldehyde with a 52% yield (0.25 g, 0.43 mmol). The experimental spectra for **C1** and **C2** are shown in the supporting information.

C1: $(C_{12}H_{17}N_2O_5V)_2$ Color yellow: FT-IR (cm^{-1}, KBr): υ(C=N) 1635, υ(V=O) 915, υ(V-O) 843 (**Fig.S1**). ^1H NMR (300 MHz, DMSO-d6, ppm): 3.37 (3H, S), 3.47-3.97 (6H, m), 4.83 (H, S), 5.51 (H, S), 6.32(H, m), 6.43 (H, d, *J* = 3 Hz), 7.44 (H, s), 8.75 (H, S). ^{13}C NMR (75 MHz, DMSO-d6, ppm): 48.35 (CH_2), 55.31(CH_3), 57.44 (CH_2), 58.35 (CH_2), 59.86 (CH_2), 102.09 (CH), 106.57(CH), 114.34 (C), 135.09 (CH), 165.61 (C), 166.93 (C), 167.55 (CH=N) (**Fig.S2**).

C2: $(C_{11}H_{15}N_2O_4V)_2$ Color yellow: FT-IR (cm^{-1}, KBr): υ(C=N) 1640, υ(V=O) 927, υ(V-O) 829. ^1H NMR (300 MHz, DMSO-d6, ppm): 3371-4.02 (6H, m), 4.58 (2H, S), 6.77 (H, d, J=3 Hz), 6.83 (H, d, J=3 Hz), 7.43 (H, d, J =3 Hz), 7.55 (H, d, J =3 Hz), 8.88 (H, S). ^{13}C NMR (75 MHz, DMSO-d6, ppm): 48.08 (CH_2), 57.36 (CH_2), 57.78 (CH_2), 58.32 (CH_2), 116.98 (CH), 119.45 (CH), 120.41 (C), 133.95 (CH), 135.46 (CH), 164.58 (C), 168.13 (CH=N) (**Fig.S3**).

2.3. X-ray crystallography

A crystal of complex **C1** was mounted on a Stoe Image Plate Diffraction system equipped with a ϕ circle goniometer, using Mo-Kα graphite monochromated radiation (λ = 0.71073 Å) with ϕ range 0-200º. The structure was solved by direct methods using the program SHELXS-2014, while the refinement and all further calculations were carried out using SHELXL-2014 [39]. The H-atoms were included in calculated positions and treated as riding atoms using the SHELX default parameters, while the non-H atoms were refined anisotropically, using a weighted full-matrix least-square on F^2. In **C1**, a methoxy group is disordered over two positions, with occupancies of 0.7 and 0.3, respectively. Crystallographic details are summarized in Table 1 and Figure 1, is drawn with ORTEP [40].

Table 1. Crystallographic and structure refinement parameters for complex **C1**.

Chemical formula	$C_{24}H_{34}N_4O_{10}V_2$
Formula weight	640.43
Crystal system	monoclinic
Space group	$P\ 2_1/c$ (no. 14)
Crystal color & shape	yellow block
Crystal size	0.22 x 0.21 x 0.18
a (Å)	10.8559(12)
b (Å)	9.5098(9)
c (Å)	13.7023(15)
β (º)	103.863(9)
V (Å^3)	1373.4(3)
Z	2
T (K)	293(2)
D_c (g.cm^{-3})	1.549
μ (mm^{-1})	0.743
Scan range (º)	$1.93 < \theta < 29.23$
Unique reflections	3715
Reflections used [I>2σ(I)]	2460
R_{int}	0.0529
Final R indices [I>2σ(I)]*	0.0378, wR_2 0.0747
R indices (all data)	0.0743, wR_2 0.0826
Goodness-of-fit	0.903
Max, Min Δρ/e (Å^{-3})	0.277, -0.279

* Structures were refined on F_0^2: $wR_2 = [\Sigma[w(F_0^2 - F_c^2)^2] / \Sigma w(F_0^2)^2]^{1/2}$, where $w^{-1} = [\Sigma(F_0^2) + (aP)^2 + bP]$ and $P = [\max(F_0^2, 0) + 2F_c^2]/3$.

CCDC-1917114 (**C1**) contains the supplementary crystallographic data for this paper. These data can be obtained free of charge at www.ccdc.cam.ac.uk/conts/retrieving.html [or from the Cambridge Crystallographic Data Centre, 12, Union Road, Cambridge CB2 1EZ, UK; fax: (internat.) +44-1223/336-033; E-mail: deposit@ccdc.cam.ac.uk].

2.4. DFT modeling

All quantum chemical calculations were performed using the Gaussian 09 program package [41]. The selected molecular geometry and vibrational wavenumbers of **C1** were optimized at the B3LYP level using the 6-31G basis set [42] which was assigned to all atoms [43]. Furthermore, to ensure that the optimized geometry is the most stable conformation, vibrational frequency calculations were used, and the calculated results showed no negative frequencies. The NMR chemical shifts have been calculated using the Gauge Including Atomic Orbital (GIAO) method with B3LYP/6-31++G(d,p) [43,44].

2.5. Antioxidant activity

The antioxidant activity was investigated by the α,α-diphenyl-β-picrylhydrazyl (DPPH) assay. The free radical scavenging activity was evaluated using a method already described [45], with slight modifications. 0.1 mL of various concentrations of **C1**, **C2**, butylated hydroxytoluene (BHT), and Quercetin were added to 0.9 mL of a methanolic solution of DPPH (60 μM). The reaction mixture was well shaken and kept at room temperature in the dark for 30 min. The absorbance of the mixture was recorded at 517 nm. The DPPH radical inhibition was calculated as follows:

DPPH radical scavenging % = [(OD control – OD sample)/OD control] × 100

Where OD control is the absorbance of blank and OD sample is the absorbance of the samples. The IC_{50} value is the inhibition concentration of the test sample that decreases 50 % of initial radical. It was calculated from the response curves of scavenging activity against the concentrations of the samples.

3. Results and discussion

3.1. Crystal structure analysis

The crystal structure of the **C1** complex is depicted in Figure 1. The structure crystallizes in monoclinic system with a space group $P2_1/c$, a = 10.8559(12) Å, b = 9.5098(9) Å, c =

13.7023(15) Å, β = 103.863(9)°, V = 1373.4(3) Å^3 and Z = 2. The reported **C2** structure also crystallizes in monoclinic system but with a space group $P2_1/n$ and a smaller volume of V = 1189(1) Å^3 due to the absence of a radical in the salicylaldehyde part [38]. Figure 1 shows that the symmetric dimer molecule has a slight octahedral distortion with a center of symmetry formed by a bridge of two oxygen atoms (O5-V1 and O5'-V1') with a distance of 1.6730 (2) Å. This distance was found to be 1.678 (2) Å in similar di-nuclear complex having a 3-ethoxy substituent in salicylaldehyde part [46], which is very close to our results. The six coordinated central vanadium (V) of each monomer is completed with the NNO donor and the V1N1 and V1N2 bonds with 2.1610(3) Å and 2.1630(3) Å, respectively. Moreover, the angles formed by O1-V1-O5 and O5-V1-O4 are 99.13(11)° and 107.19(14)°, respectively. They correlate with those found in reference [46] which were 98.86(10)° and 107.58(12)°. Similarly, bond lengths and angles described in other di-nuclear vanadium complex structures [47–49] were found in accordance with the titled complex.

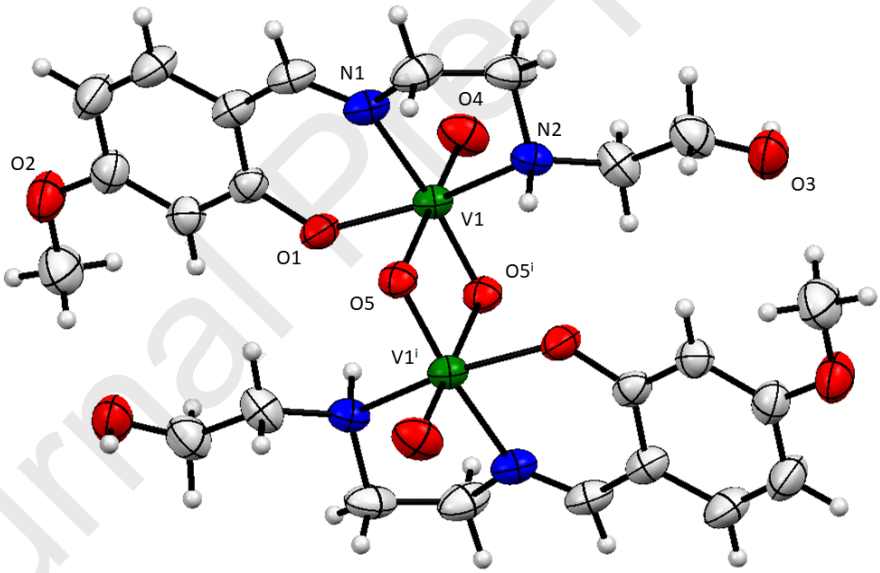

Fig.1. Molecular structure of **C1** at 50% probability level ellipsoids, with only one orientation of the disordered terminal methoxy group being presented (i = 1-x, -y, -z).

3.2. Computational investigations and DFT calculations

The geometry of the complex **C1** was obtained in a singlet ground state by DFT at B3LYP/6-31G. Some significant bond lengths and bond angles of the optimized geometry of **C1** along with their corresponding X-ray data are given in **Table 2**.

Table 2 . Selected X-ray and calculated bond distances (Å) and angles (°) for **C1**

	Experimental X-ray	Calculated
Bonds		
V1-V2	3.119 (7)	3.169
O1-V1	1.907 (14)	1.928
V1-O4	1.619 (15)	1.621
V1-O5	1.669 (13)	1.680
C1-O1	1.331 (2)	1.347
C3-O2	1.362 (3)	1.383
N1-V1	2.159 (16)	2.159
N2-V1	2.162 (17)	2.196
C7-N1	1.284 (3)	1.299
C1-C6	1.411 (3)	1.426
Angles		
V1-O1-C1	132.07 (13)	130.24
C3-O2-C12	117.90 (17)	119.16
O5-V1-O1	99.13 (6)	99.33
O4-V1-O5	107.19 (8)	108.77
N2-C10-C11	115.16 (19)	114.36

3.3. IR *Spectral study*

The IR spectra of **C1** was computed at the B3LYP/6-31G level of theory in the region between 400 and 4000 cm^{-1}. The calculated data was compared with the observed values and the results are listed in **Table 3**. The experimental FT-IR spectrum is shown in **Figure S.1**.

Table 3. Vibrational frequency assignments of **C1** with experimental and calculated DFT methods.

Assignments	Experimental	Calculated
υ(C-H_{sp3})	2940	2938
υ(C=N)	1635	1684
υ(V=O)	915	905

The C=N stretch observed at 1635 cm^{-1} is in accordance with results from previous report [50] and it was found to be in good agreement with the computed value at 1684 cm^{-1}. The absorption band experimentally observed at 915 cm^{-1} and calculated at 905 cm^{-1} is associated with the V=O vibration [51].

3.4. NMR spectra calculations

^{1}H and ^{13}C NMR chemical shifts of **C1** complex were carried out at the B3LYP/6-31G++(d,p) using GIAO approach in solvent phase. The calculations were performed in DMSO-d_6 solvent by using C-PCM formalism, and the selected shifts were compared with the experimental values as illustrated in **Table 4**. The curves between the predicted and the experimental data are shown in Figure 3. The correlation coefficients R^2 of 99.05% and 98.51% for the selected ^{1}H and ^{13}C NMR chemical shifts, respectively, show that experimental NMR data are consistent with the computed values from the optimized structure of **C1**.

Table 4. Selected experimental and theoretical ^{1}H and ^{13}C NMR shifts (ppm) of **C1**.

^{1}H NMR chemical shifts (ppm)			^{13}C NMR chemical shifts (ppm)		
Atoms	Experimental (DMSO)	Calculated DFT/B3LYP (ppm)	Atoms	Experimental (DMSO)	Calculated DFT/B3LYP (ppm)
H2	7.44	7.08	C1	167.55	166.55
H2N	-	4.60	C2	106.57	104.31
H4	4.83	4.84	C3	166.93	168.75
H5	6.32	6.19	C5	135.09	132.43
H7	6.43	6.77	C6	102.09	100.53
H8	3.97	4.08	C7	165.61	157.52
H10	2.33	2.34	C8	48.35	50.60

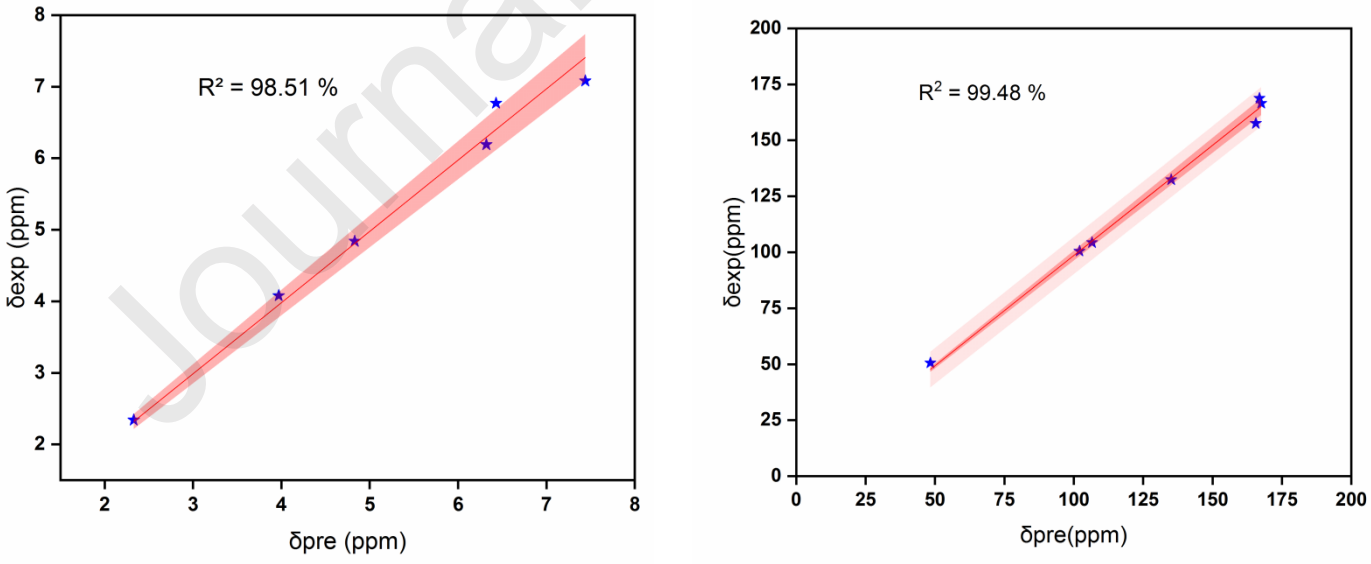

Fig. 3. Correlation curves between the predicted and experimental ^{1}H NMR (left) and ^{13}C NMR (right) chemical shifts for **C1**.

3.5. Orbital analysis and HOMO-LUMO gap

The highest occupied molecular orbital (HUMO) associated with electron-donating potential and the lowest unoccupied molecular orbital related to electron affinity [52] are important in the quantum chemistry [53]. The difference between these two parameters (HUMO-LUMO gap) can reveal the chemical reactivity of molecules. Contour plots of the HOMO and LUMO orbitals for **C1** and **C2** are shown in Figure 4 and Figure S4, respectively. The energy gap between HOMO and LUMO molecular orbitals of **C1** and **C2** was found to be 4.02 and 4.13 eV, respectively, with ligand to metal charge transfer (LMCT).

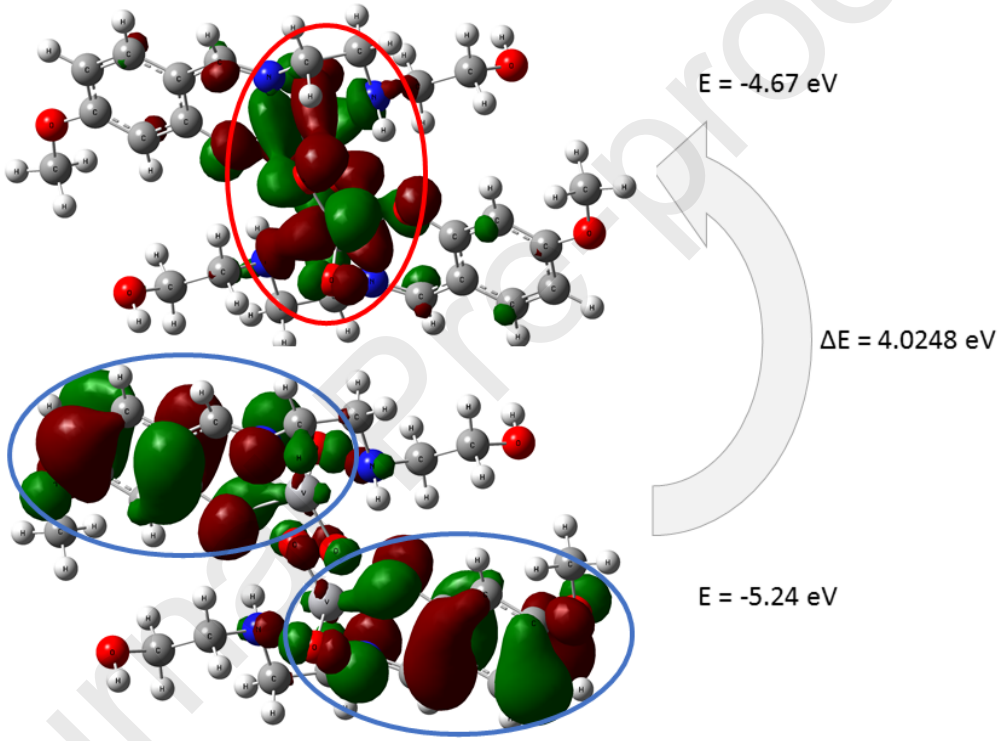

Fig .4. Isodensity plots of HOMO and LUMO and their energies obtained at B3LYP/6-31G level for **C1**.

3.6. Hirshfeld surface and EPS analyses

The Hirshfeld surface (HS) [54], which is the space occupied by a single molecule in a crystal motif in order to divide the crystal electron density into molecular fragments, was computed using the Crystal Explorer 17.5 program [55]. HS, combined with the two-dimensional calculation of fingerprint plots, allow identification of the close contacts of each atom calculated by the normalized contact distance d_{norm} with the nearest nucleus internal (d_i)

and external (d_e) distances to the surface [56]. Additionally, the electrostatic potential surface (EPS) was defined at the B3LYP/6-311+G(d) level of theory.

HS analysis and EPS (**Fig.5**) provide 3D presentations of intermolecular interactions between different contacts of each atom. A red spot over the HS indicates the interaction that involved hydrogen bonding, whereas in the EPS map, the negative electrostatic potential appears in the red area (hydrogen acceptors), and the positive electrostatic potential (hydrogen donor) appears in blue.

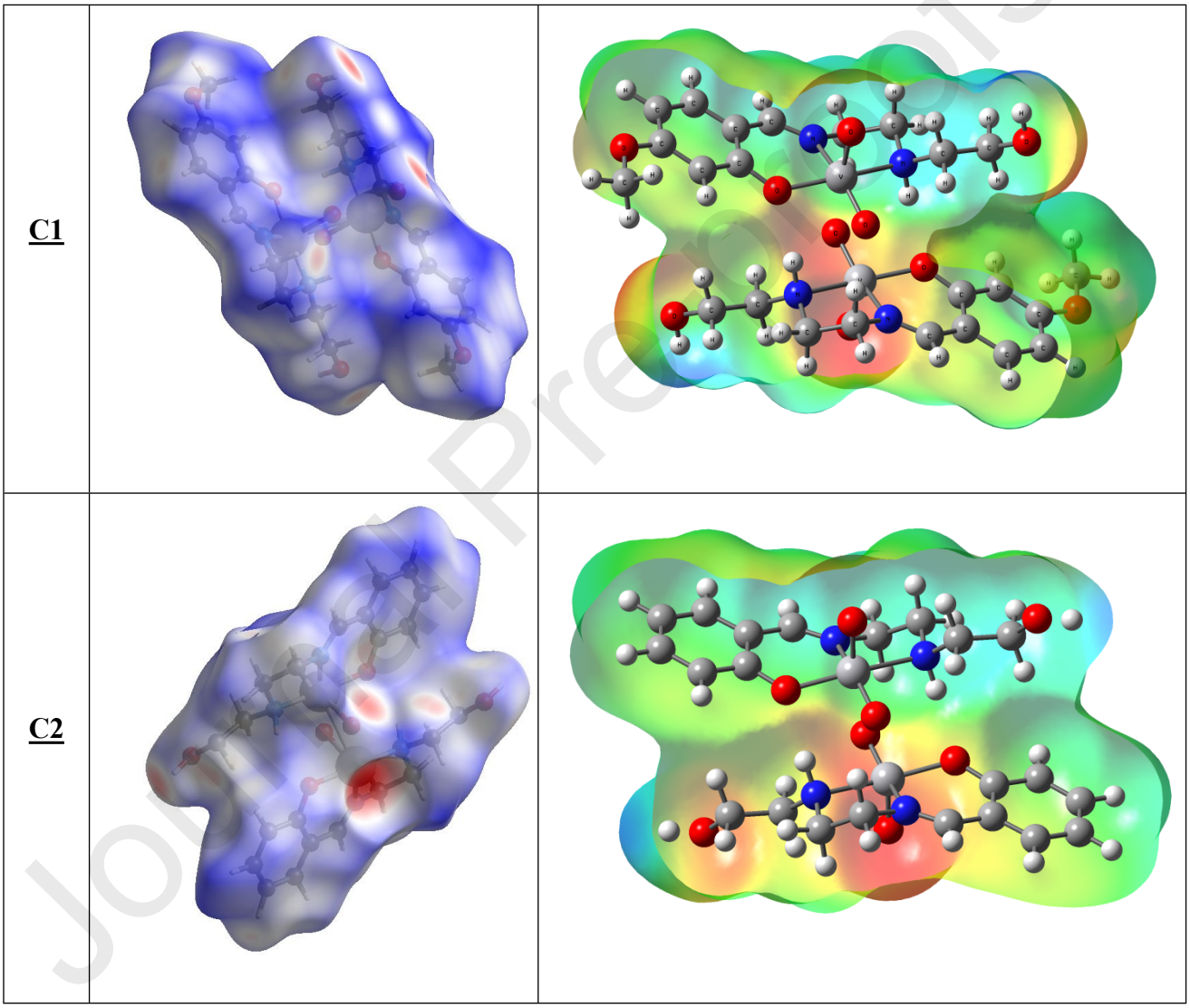

Fig. 5. HS mapping surface (left) and EPS (right) for **C1** and **C2**.

Therefore, the inter-contacts over the HS are shown using 2D-fingerprint scatter plots (**Fig. 6**). In these scatter plots, d_e corresponds to the closest external contacts (i.e., external distance) from a given point of the HS, and d_i to the closest internal distance. Three colors are revealed in the map; blue for some occurrence, white if no occurrence, and green for frequent

occurrence [54]. The major intermolecular contacts including reciprocal interactions are H···H, O···H, and C···H contacts with 47.8 %, 30.2 %, and 16.6 %, respectively for **C1** and the corresponding ones for **C2** are 47.1 %, 26.7 % and 18 %, respectively. The O···H contacts are represented by two spikes in the left region (donor) and a spike in the right region (acceptor) of the 2D-fingerprint plots. These inter-contacts are significantly medium and important in the molecular packing of the studied complexes.

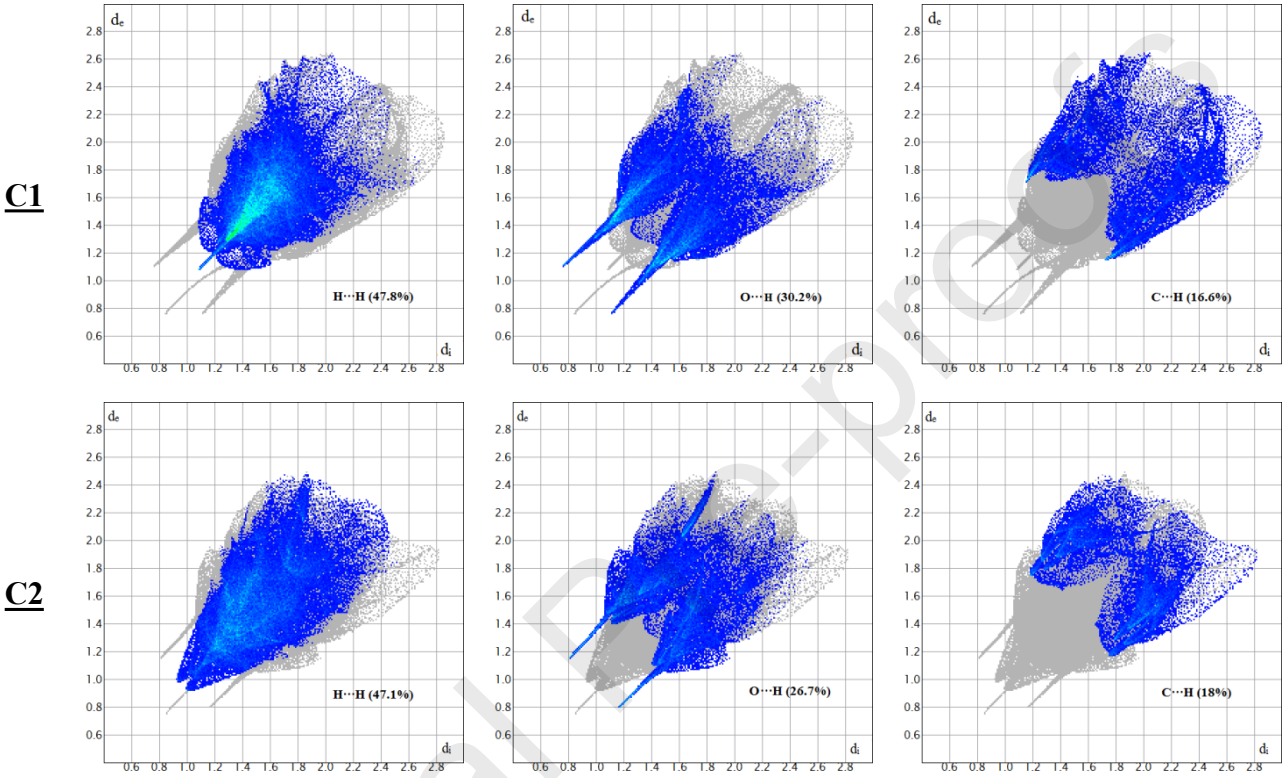

Fig. 6. 2D-Fingerprint plots of the major inter-contacts in **C1** and **C2**.

3.7. Antioxidant activity

Several methods (FRAP, ABTS, H_2O_2, FIC, DPPH, etc.) have been developed to assess the antioxidant activity of different organic compounds [57]. Some of these methods estimate the capacity of the bioactive compounds to scavenge specific radicals, chelate ions, or inhibit peroxidation of lipids [58].

In the present study, the DPPH assay was used to estimate the antioxidant activity of **C1** and **C2** complexes using BHT and quercetin as antioxidant standards. It shows that H-atom transfer is involved in the radical scavenging process. Therefore, the antioxidant compounds donate the hydrogen to a DPPH radical and convert it into DPPH-H. As shown in Table 5, the complex **C1** which possesses one hydroxyl group in the ortho position exhibited the strongest scavenging activity of DPPH with an IC_{50} value of 1.446 mg/mL. This was followed by the complex **C2** with a value of IC_{50} equal to 1.572 mg/mL. According to these results, **C1** and

C2 complexes are less active than BHT and quercetin. Although, the antioxidant standards are the most potent scavengers of the free radical DPPH•, this does not prevent the studied compounds from being active and having a considerable antiradical capacity. The efficiency of the ortho and para compounds is in part due to the regeneration of another compound [59] or the stabilization of the aryloxyl radical by hydrogen bonding [60]. Moreover, it has been reported that the ortho-methoxy substitution also stabilizes the aryloxyl radical by electron donation [61] and therefore increases the antioxidant and the antiradical efficiencies. The bond dissociation energies of the O–H bonds are also important criteria in evaluating the antioxidant activity, because the weaker the OH bond the easier will be the reaction of free radical inactivation [62,63].

Table 5. Antioxidant activity of **C1** and **C2** complexes.

Entry	Compounds	DPPH assay (mg/mL)
1	**C1**	1.446 ± 0.012
2	**C2**	1.572 ± 0.011
3	**BHT**	0.060 ± 0.001
4	**Quercetin**	0.040 ± 0.001

Values are presented as means ± standard deviation (SD) of three replications

4. Conclusion

In this report, the vanadium (V) di-nuclear complex **C1** was synthesized from a Schiff base (L_1H) tridentate bearing NNO donors and $VOSO_4$. The single crystal X-ray diffraction confirmed the presence of a bridge formed by an oxo group in the dimer structure. The complex has been fully characterized by FT-IR, ^1H, and ^{13}C NMR. The prediction of the structural parameters and vibrational frequencies using DFT method are in accordance with the experimental results. The comparison between **C1** and **C2** complexes has indicated that both structures crystallized in a monoclinic system. Moreover, it has been found that the intermolecular interactions over the Hirshfeld surface showed that the major interactions in both structures are slightly the same. DPPH free radical scavenging was used as a simple, rapid, and cheap method to determine the antioxidant activity, and the results have clearly shown that the radical scavenging activity of **C1** and **C2** is much higher than BHT and quercetin.

Acknowledgements

The authors would like to thank Professor Bruno Therrien at Institute of Chemistry, University of Neuchâtel for performing the X-ray diffraction characterization of the sample.

Declaration of Interest

The authors declare that there are no conflicts of interest.

References

[1] S. Matsunaga, M. Shibasaki, Recent advances in cooperative bimetallic asymmetric catalysis: dinuclear Schiff base complexes, Chem. Commun. 50 (2014) 1044–1057. https://doi.org/10.1039/C3CC47587E.

[2] H. Hosseini-Monfared, A. Farrokhi, S. Alavi, P. Mayer, Synthesis, structure and catalytic activity of an oxo-bridged dinuclear oxovanadium complex of an isonicotinohydrazide ligand, Transit. Met. Chem. 38 (2013) 267–273. https://doi.org/10.1007/s11243-012-9687-z.

[3] S. Biswas, P. Roy, T.K. Mondal, Synthesis of palladium(II) complex with NNS donor Schiff base ligand via C S bond cleavage: X-ray structure, electrochemistry and DFT computation, J. Mol. Struct. 1142 (2017) 110–115. https://doi.org/10.1016/j.molstruc.2017.04.044.

[4] F. Heidari, S.J.A. Fatemi, S. Yousef Ebrahimipour, H. Ebrahimnejad, J. Castro, M. Dušek, V. Eigner, Six-coordinate oxo-vanadium(V) dimer complex with methoxy bridging: Synthesis, crystal structure, biological activity and molecular docking, Inorg. Chem. Commun. 76 (2017) 1–4. https://doi.org/10.1016/j.inoche.2016.11.015.

[5] E.T. Saka, N. Kahriman, (E)-4-(4-(3-(2-fluoro-5-(trifluoromethyl)phenyl)acryloyl) phenoxy) Substituted Co(II) and Cu(II) phthalocyanines and their catalytic activities on the oxidation of phenols, J. Organomet. Chem. (2019). https://doi.org/10.1016/j.jorganchem.2019.05.012.

[6] S. Tabassum, S. Amir, F. Arjmand, C. Pettinari, F. Marchetti, N. Masciocchi, G. Lupidi, R. Pettinari, European Journal of Medicinal Chemistry Mixed-ligand Cu (II) e vanillin Schiff base complexes ; effect of coligands on their DNA binding , DNA cleavage , SOD mimetic and anticancer activity, Eur. J. Med. Chem. 60 (2013) 216–232. https://doi.org/10.1016/j.ejmech.2012.08.019.

[7] S.N. Pandeya, D. Sriram, G. Nath, E. DeClercq, Synthesis, antibacterial, antifungal and anti-HIV activities of Schiff and Mannich bases derived from isatin derivatives and N-[4-(4′-chlorophenyl)thiazol-2-yl] thiosemicarbazide, Eur. J. Pharm. Sci. 9 (1999) 25–31. https://doi.org/10.1016/S0928-0987(99)00038-X.

[8] A. Palanimurugan, A. Kulandaisamy, DNA, in vitro antimicrobial/anticancer activities and biocidal based statistical analysis of Schiff base metal complexes derived from salicylalidene-4-imino-2,3-dimethyl-1-phenyl-3-pyrazolin-5-one and 2-aminothiazole, J. Organomet. Chem. (2018). https://doi.org/10.1016/j.jorganchem.2018.02.051.

[9] W.H. Mahmoud, M.M. Omar, F.N. Sayed, G.G. Mohamed, Synthesis, characterization, spectroscopic and theoretical studies of transition metal complexes of new nano Schiff base derived from L-histidine and 2-acetylferrocene and evaluation of biological and anticancer activities, Appl. Organomet. Chem. 32 (2018) e4386. https://doi.org/10.1002/aoc.4386.

[10] G.B. Bagihalli, P.G. Avaji, S.A. Patil, P.S. Badami, Synthesis, spectral

characterization, in vitro antibacterial, antifungal and cytotoxic activities of Co(II), Ni(II) and Cu(II) complexes with 1,2,4-triazole Schiff bases, Eur. J. Med. Chem. 43 (2008) 2639–2649. https://doi.org/10.1016/j.ejmech.2008.02.013.

[11] Z.G. Hong, X.M. Zhang, T.X. Wu, C. Zheng, B. Luo, J. Tang, F.P. Huang, D. Yao, H.D. Bian, Synthesis, crystal structures and antioxidant activities of water-soluble salicylaldehyde Schiff base complexes, Polyhedron. 159 (2019) 355–364. https://doi.org/10.1016/j.poly.2018.12.014.

[12] A. Pejović, A. Minić, J. Jovanović, M. Pešić, D.I. Komatina, I. Damljanović, D. Stevanović, V. Mihailović, J. Katanić, G.A. Bogdanović, Synthesis, characterization, antioxidant and antimicrobial activity of novel 5-arylidene-2-ferrocenyl-1,3-thiazolidin-4-ones, J. Organomet. Chem. 869 (2018) 1–10. https://doi.org/10.1016/j.jorganchem.2018.05.014.

[13] M. Pourkhosravani, S. Dehghanpour, F. Farzaneh, S. Sohrabi, Designing new catalytic nanoreactors for the regioselective epoxidation of geraniol by the post-synthetic immobilization of oxovanadium (IV) complexes on a Zr (IV)-based metal–organic framework, React. Kinet. Mech. Catal. 122 (2017) 961–981. https://doi.org/10.1007/s11144-017-1253-4.

[14] J. Krakowiak, D. Lundberg, I. Persson, A Coordination Chemistry Study of Hydrated and Solvated Cationic Vanadium Ions in Oxidation States +III, +IV, and +V in Solution and Solid State, Inorg. Chem. (2012). https://doi.org/10.1021/ic300202f.

[15] D.C. Crans, J.J. Smee, E. Gaidamauskas, L. Yang, The Chemistry and Biochemistry of Vanadium and the Biological Activities Exerted by Vanadium Compounds, Chem. Rev. 104 (2004) 849–902. https://doi.org/10.1021/cr020607t.

[16] H. Sakurai, Y. Kojima, Y. Yoshikawa, K. Kawabe, H. Yasui, Antidiabetic vanadium(IV) and zinc(II) complexes, Coord. Chem. Rev. 226 (2002) 187–198. https://doi.org/10.1016/S0010-8545(01)00447-7.

[17] R.R. Eady, Current status of structure function relationships of vanadium nitrogenase, Coord. Chem. Rev. 237 (2003) 23–30. https://doi.org/10.1016/S0010-8545(02)00248-5.

[18] D. Gambino, Potentiality of vanadium compounds as anti-parasitic agents, Coord. Chem. Rev. 255 (2011) 2193–2203. https://doi.org/10.1016/j.ccr.2010.12.028.

[19] D. Rehder, G. Santoni, G.M. Licini, C. Schulzke, B. Meier, The medicinal and catalytic potential of model complexes of vanadate-dependent haloperoxidases, Coord. Chem. Rev. 237 (2003) 53–63. https://doi.org/10.1016/S0010-8545(02)00300-4.

[20] G. Romanowski, J. Kira, M. Wera, Vanadium(V) complexes with chiral tridentate Schiff base ligands derived from 1S,2R(+)-2-amino-1,2-diphenylethanol and with acetohydroxamate co-ligand: Synthesis, characterization and catalytic activity in the oxidation of prochiral sulfides and olefins, J. Mol. Catal. A Chem. 381 (2014) 148–160. https://doi.org/10.1016/j.molcata.2013.10.011.

[21] G. Grivani, V. Tahmasebi, A.D. Khalaji, K. Fejfarová, M. Dušek, Synthesis, characterization and crystal structure determination of a new vanadium (IV) Schiff base complex (VOL2) and investigation of its catalytic activity in the epoxidation of cyclooctene, Polyhedron. 51 (2013) 54–60. https://doi.org/10.1016/j.poly.2012.12.008.

[22] C. Cordelle, D. Agustin, J. Daran, R. Poli, Oxo-bridged bis oxo-vanadium(V) complexes with tridentate Schiff base ligands (VOL)2O (L=SAE, SAMP, SAP): Synthesis, structure and epoxidation catalysis under solvent-free conditions, Inorganica Chim. Acta. 364 (2010) 144–149. https://doi.org/10.1016/j.ica.2010.09.021.

[23] H. Hosseini Monfared, S. Kheirabadi, N. Asghari Lalami, P. Mayer, Dioxo- and oxovanadium(V) complexes of biomimetic hydrazone ONO and NNS donor ligands: Synthesis, crystal structure and catalytic reactivity, Polyhedron. 30 (2011) 1375–1384.

https://doi.org/10.1016/j.poly.2011.02.005.

[24] M. Sutradhar, A.J.L. Pombeiro, Coordination chemistry of non-oxido, oxido and dioxidovanadium(IV/V) complexes with azine fragment ligands, Coord. Chem. Rev. 265 (2014) 89–124. https://doi.org/10.1016/j.ccr.2014.01.007.

[25] S. Mondal, M. Mukherjee, K. Dhara, S. Ghosh, J. Ratha, P. Banerjee, A.K. Mukherjee, Supramolecular architecture in an oxovanadium(V)-schiff base complex: Synthesis, Ab initio structure determination from X-ray powder diffraction, DNA binding and cleavage activity, Cryst. Growth Des. 7 (2007) 1716–1721. https://doi.org/10.1021/cg060753i.

[26] Y.M. Cui, Y.J. Cai, W. Chen, Synthesis and structures of 3-chloro-N′-(2-hydroxy-benzylidene) benzohydrazide and its oxovanadium(V) complex, J. Coord. Chem. 64 (2011) 1385–1392. https://doi.org/10.1080/00958972.2011.571680.

[27] E.B. Seena, N. Mathew, M. Kuriakose, M.R.P. Kurup, Synthesis, spectral and EPR studies of oxovanadium(IV) complexes incorporating tridentate ONO donor hydrazone ligands: Structural study of one oxovanadium(V) complex, Polyhedron. 27 (2008) 1455–1462. https://doi.org/10.1016/j.poly.2008.01.020.

[28] N.R. Sangeetha, V. Kavita, S. Wocadlo, A.K. Powell, S. Pal, Vanadium(v) complexes of O,N,O-donor tridentate ligands containing the {VvO(OMe)}2+ unit: Syntheses, structures and properties, J. Coord. Chem. 51 (2000) 55–66. https://doi.org/10.1080/00958970008047078.

[29] Z.L. You, D.H. Shi, J.C. Zhang, Y.P. Ma, C. Wang, K. Li, Synthesis, structures, and urease inhibitory activities of oxovanadium(V) complexes with Schiff bases, Inorganica Chim. Acta. 384 (2012) 54–61. https://doi.org/10.1016/j.ica.2011.11.039.

[30] J.A.L. da Silva, J.J.R.F. da Silva, A.J.L. Pombeiro, Oxovanadium complexes in catalytic oxidations, Coord. Chem. Rev. 255 (2011) 2232–2248. https://doi.org/10.1016/j.ccr.2011.05.009.

[31] B. Mondal, M.G.B. Drew, R. Banerjee, T. Ghosh, Chemistry of mixed-ligand methoxy bonded oxidovanadium(V) complexes with a family of hydrazone ligands containing VO3+ core and their substituent controlled methoxy-bridged dimeric forms, Polyhedron. 27 (2008) 3197–3206. https://doi.org/10.1016/j.poly.2008.07.004.

[32] M.R. Maurya, S. Agarwal, M. Abid, A. Azam, C. Bader, M. Ebel, D. Rehder, Synthesis, characterisation, reactivity and in vitro antiamoebic activity of hydrazone based oxovanadium(iv), oxovanadium(v) and -bis(oxo) bis{oxovanadium(v)} complexes, Dalt. Trans. (2006) 937–947. https://doi.org/10.1039/b512326g.

[33] D.F. Back, C.R. Kopp, G. Manzoni de Oliveira, P.C. Piquini, New oxidovanadium(V) complexes of the cation [VO]3+: Synthesis, structural characterization and DFT studies, Polyhedron. 36 (2012) 21–29. https://doi.org/10.1016/j.poly.2012.01.015.

[34] R. Haunschild, A. Barth, W. Marx, Evolution of DFT studies in view of a scientometric perspective, J. Cheminform. 8 (2016) 52. https://doi.org/10.1186/s13321-016-0166-y.

[35] A. Coletti, P. Galloni, A. Sartorel, V. Conte, B. Floris, Salophen and salen oxo vanadium complexes as catalysts of sulfides oxidation with H2O2: Mechanistic insights, Catal. Today. 192 (2012) 44–55. https://doi.org/10.1016/j.cattod.2012.03.032.

[36] Y. Kitagawa, T. Matsui, N. Yasuda, H. Hatake, T. Kawakami, S. Yamanaka, M. Nihei, M. Okumura, H. Oshio, K. Yamaguchi, DFT calculations of effective exchange integrals at the complete basis set limit on oxo-vanadium ring complex, Polyhedron. 66 (2013) 97–101. https://doi.org/10.1016/j.poly.2013.02.040.

[37] A. Hasnaoui, I. Hdoufane, R. Idouhli, B. Therrien, M. Ait Ali, L. El Firdoussi, Crystal structure of {N-(2-hydroxyethylamino) ethylsalicylaldiminato]-palladium(II) chloride}: Synthesis, X-ray structure, electrochemistry, DFT and TDDFT studies, J. Mol. Struct. 1176 (2019) 703–710. https://doi.org/10.1016/j.molstruc.2018.08.111.

[38] M. Mikuriya, K. Matsunami, Synthesis and structural characterization of a series of transition metal complexes with a tetradentate Schiff-base ligand derived from salicylaldehyde and 2-(2-aminoethylamino)ethanol, Mater. Sci. Pol. 23 (2005) 773–792.

[39] G.M. Sheldrick, SHELXT – Integrated space-group and crystal-structure determination, Acta Crystallogr. Sect. A Found. Adv. 71 (2015) 3–8. https://doi.org/10.1107/S2053273314026370.

[40] L.J. Farrugia, WinGX suite for small-molecule single-crystal crystallography, J. Appl. Crystallogr. 32 (1999) 837–838. https://doi.org/10.1107/S0021889899006020.

[41] G.S. M.J. Frisch, G.W. Trucks, H.B. Schlegel, G.E. Scuseria, M.A. Robb, J.R. Cheeseman, J. V. Barone, B. Mennucci, G.A. Petersson, H. Nakatsuji, M. Caricato, H.P.H. X. Li, A.F. Izmaylov, M. Bloino, G. Zheng, J.L. Sonnenberg, M. Hada, M. Ehara, K. Toyota, R. Fukuda, J. Hasegawa, M. Ishida, T. Nakajima, Y. Honda, O. Kitao, H. Nakai, T. Vreven, J.A.M. Jr., J.E. Peralta, F. Ogliaro, J.R. Bearpark, J.J. Heyd, E. Brothers, K.N. Kudin, V.N. Staroverov, R. Kobayashi, Normand, J.E. Rendell, K.A.J.C. Burant, S.S. Iyengar, J. Tomasi, M. Cossi, N. Rega, J.M. Millam, M. Klene, A.J. Knox, J.B. Cross, V. Bakken, C. Adamo, J. Jaramillo, R. Gomperts, R.E. Stratmann, O. Yazyev, G.A. Austin, R. Cammi, C. Pomelli, J.W. Ochterski, R.L. Martin, K. Morokuma, V.G. Zakrzewski, J. Voth, P. Salvador, J.J. Dannenberg, S. Dapprich, A.D.D.O. Farkas, J.B. Foresman, J.V. Ortiz, W.C. Cioslowski, D.J. Fox, Fox, ., No Title, Gaussian 09, Revis. D.01, Gaussian, Inc. (2009).

[42] R.G.P. C. Lee, W. Yang, Development of the Colle-Salvetti correlation-energy formula into a functional of the electron density, Phys. Rev. B. 37 (1988) 785–789.

[43] A.D. Becke, Density-functional thermochemistry. III. The role of exact exchange, J. Chem. Phys. 98 (1993) 5648–5652. https://doi.org/10.1063/1.464913.

[44] C. Lee, W. Yang, R.G. Parr, Development of the Colle-Salvetti correlation-energy formula into a functional of the electron density, Phys. Rev. B. 37 (1988) 785–789. https://doi.org/10.1103/PhysRevB.37.785.

[45] R. Tundis, F. Menichini, M. Bonesi, F. Conforti, G. Statti, F. Menichini, M.R. Loizzo, LWT - Food Science and Technology Antioxidant and hypoglycaemic activities and their relationship to phytochemicals in Capsicum annuum cultivars during fruit development, LWT - Food Sci. Technol. 53 (2013) 370–377. https://doi.org/10.1016/j.lwt.2013.02.013.

[46] F.-M. Wang, Di-μ-oxido-bis[(2-ethoxy-6-{[2-(2-hydroxyethylamino) ethylimino] methyl}phenolato-κ 3 N , N ′, O 1)oxidovanadium(V)], Acta Crystallogr. Sect. E Struct. Reports Online. 68 (2012) m26–m27. https://doi.org/10.1107/S160053681105094X.

[47] R.N. Patel, Y.P. Singh, Y. Singh, R.J. Butcher, J.P. Jasinski, New di-μ-oxidovanadium(V) complexes with NNO donor Schiff bases: Synthesis, crystal structures and electrochemical studies, Polyhedron. 133 (2017) 102–109. https://doi.org/10.1016/j.poly.2017.05.028.

[48] M. Ghorbani, A.D. Khalaji, N. Feizi, A. Akbari, V. Eigner, M. Dusek, μ 2 -Oxido bridged dinuclear vanadium(V) complex: Synthesis and characterization, J. Mol. Struct. 1130 (2017) 442–446. https://doi.org/10.1016/j.molstruc.2016.10.024.

[49] S.-J. Li, K. Li, X.-Y. Qiu, X.-J. Yao, Two New Isomeric Di-μ-oxo Bis[oxovanadium(V)] Complexes Containing Schiff Base Ligands, J. Chem. Crystallogr. 42 (2012) 879–883. https://doi.org/10.1007/s10870-012-0330-9.

[50] R.J.B. R. N. Patela, Yogendra Pratap Singha, Yogendra Singha, New di-μ-oxidovanadium(V) complexes with NNO donor Schiff bases: Synthesis, crystal structures and electrochemical studies, 2 (2017) 879–883.

https://doi.org/10.1016/j.poly.2017.05.028.
[51] M.R. Maurya, N. Chaudhary, F. Avecilla, P. Adão, J. Costa Pessoa, Oxidovanadium(IV) and dioxidovanadium(V) complexes of hydrazones of 2-benzoylpyridine and their catalytic applications, Dalt. Trans. 44 (2015) 1211–1232. https://doi.org/10.1039/C4DT02474E.
[52] R.G. Pearson, Absolute Electronegativity and Hardness: Applications to Organic Chemistry, J. Org. Chem. 57 (1989) 1423–1430.
[53] K. Fukui, Role of Frontier Orbitals in Chemical Reactions, Am. Assoc. Adv. Sci. Stable. 218 (2019) 747–754.
[54] M.A. Spackman, D. Jayatilaka, Hirshfeld surface analysis, CrystEngComm. 11 (2009) 19–32. https://doi.org/10.1039/B818330A.
[55] M.J. Turner, J.J. McKinnon, S.K. Wolff, D.J. Grimwood, P.R. Spackman, D. Jayatilaka, M.A. Spackman, CrystalExplorer17.5, (2017).
[56] J.J. McKinnon, D. Jayatilaka, M.A. Spackman, Towards quantitative analysis of intermolecular interactions with Hirshfeld surfaces, Chem. Commun. (2007) 3814. https://doi.org/10.1039/b704980c.
[57] I.M.C. Iena, N. Mariana, T. Cristian, I.M. Popescu, C. Adina, Antioxidant Activity Evaluation of Some Novel 2- Hydroxy-Benzamides Derivatives, (2015) 6–9.
[58] J. Lü, P.H. Lin, Q. Yao, C. Chen, Chemical and molecular mechanisms of antioxidants : experimental approaches and model systems, 14 (2010) 840–860. https://doi.org/0.1111/j.1582-4934.2009.00897.x.
[59] W. Brand-Williams, M.E. Cuvelier, C. Berset, Respostas Perceptivas E, LWT - Food Sci. Technol. 28 (1995) 25–30. https://doi.org/10.1016/S0023-6438(95)80008-5.
[60] J. Pokorny, Major factors affecting th autoxidation in lipids.Ed. In : Chan, H. (Ed), autoxidation of Unsaturated Lipids, Acad. Press. (1987) 141–206.
[61] J.F. McMurry, Wound healing with diabetes mellitus. Better glucose control for better wound healing in diabetes, Surg. Clin. North Am. 64 (1984) 769–778. https://doi.org/10.1016/S0039-6109(16)43393-1.
[62] L.A. Wright, E.G. Hope, G.A. Solan, W.B. Cross, K. Singh, O,N,N-Pincer ligand effects on oxidatively induced carbon–chlorine coupling reactions at palladium, Dalt. Trans. 44 (2015) 6040–6051. https://doi.org/10.1039/C5DT00062A.
[63] M. Mohammadpour, A. Sadeghi, A. Fassihi, L. Saghaei, A. Movahedian, M. Rostami, Synthesis and antioxidant evaluation of some novel orthohydroxypyridine- 4-one iron chelators, Res. Pharm. Sci. 7 (2012) 171–179.

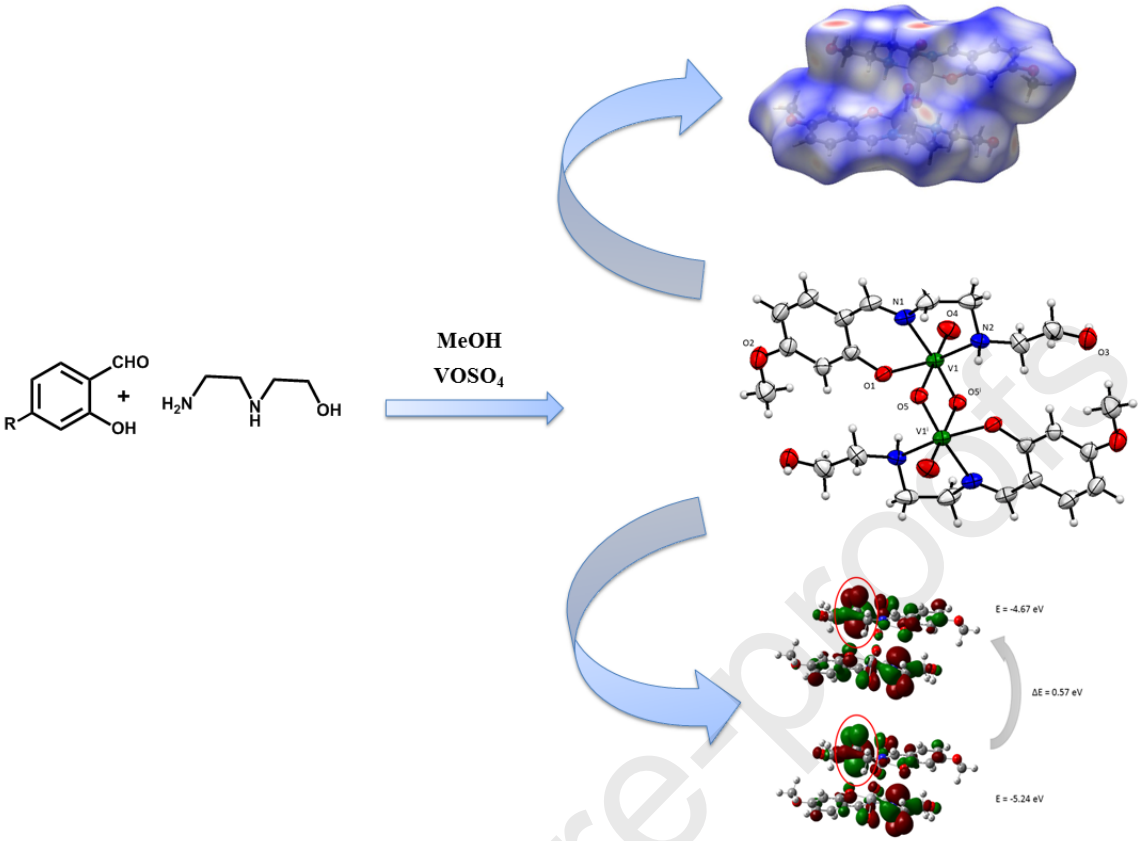

Highlights

- Synthesis of new di-μ-oxidovanadium(V) complexes [(LH)VO(μ-O)$_2$VO(LH)].
- The complexes were characterized by ^{1}H, ^{13}C NMR, FT-IR and confirmed by single-crystal X-ray diffraction.
- Computational studies using density functional theory (DFT) method were computed.
- Hirshfeldsurfaces analysis were applied to observethe intermolecular interactions in the [(LH)VO(μ-O)$_2$VO(LH)].
- Antioxydant activity of the titled products were investigated.

Marrakech, October 07th 2019

InorganicaChimica Acta

Subject: REVISION OF OUR MANUSCRIPT FOR PUBLICATION

Manuscript Title: "**Di-µ-oxidovanadium(V) di-nuclear complexes: Synthesis, X-ray, DFT modeling, Hirshfeld surface analysis and Antioxidant activity**"

Ali Hasnaoui [1], Ismail Hdoufane [2], Abderrahim Alahyane [3], Abdallah Nayad [1], Driss Cherqaoui [2], Mustapha Ait Ali [1] and Larbi El Firdoussi [1*]

Manuscript ID: ***ICA_2019_777***

Declaration of Interest

The authors declare that there are no conflicts of interest.

Di-µ-oxidovanadium(V) di-nuclear complexes: Synthesis, X-ray, DFT modeling, Hirshfeld surface analysis and Antioxidant activity

Ali Hasnaoui[1], Ismail Hdoufane[2], AbderrahimAlahyane[3], AbdallahNayad[1], DrissCherqaoui[2], Mustapha Ait Ali[1]and Larbi El Firdoussi[1*]

[1]Equipe de Chimie de Coordination et de Catalyse, Département de Chimie, Université Cadi Ayyad, Faculté des Sciences Semlalia, BP 2390, Marrakech, Morocco ;
[2] Laboratory of Molecular Chemistry, Department of Chemistry, Faculty of SciencesSemlalia, Cadi Ayyad University of Marrakech, BP 2390, Morocco;
[3] Food Sciences Laboratory, Department of Biology, Faculty of Sciences-Semlalia, Cadi Ayyad University of Marrakech, P.O. Box 2390, Morocco.

* Corresponding author.

ABSTRACT

In this work, two di-µ-oxidovanadium(V) complexes, $[(L_1H)VO(\mu\text{-}O)]_2$ (**C1**) and $[(L_2H)VO(\mu\text{-}O)]_2$ (**C2**), with tridentate Schiff base ligands, [N-(2-hydroxyethylamino)ethyl]-5-methoxysalicylaldimine (L_1H) and 2-[(2-(2-Hydroxyethylamino) ethylimino)methyl] phenol (L_2H), respectively, were prepared and characterized by various spectroscopic techniques. The X-ray diffraction of **C1** showed six-coordinate vanadium in a distorted octahedral geometry with the imine, phenolate and amine donors of the ligand and two oxo-group bonds. Density functional theory (DFT) was carried out using B3LYP level with the 6-31G basis set in order to predict the molecular structure of **C1**, delineate its vibrational wavenumbers and define the theoretical NMR shifts, which were performed with the GIAO approach. Thereafter, Hirshfeld surface (HS) and 2D fingerprint analysis were used to investigate the intermolecular contacts in the **C1** complex. The DPPH free radical scavenging assay was used to evaluate the antioxidant activity of both **C1** and **C2** complexes.